Intermedin$_{1\text{-}53}$ enhances angiogenesis and attenuates adverse remodeling following myocardial infarction by activating AMP-activated protein kinase

KANKAI CHEN[*], MEILING YAN[*], YONGGUANG LI,
ZHIFENG DONG, DONG HUANG, JINGBO LI and MENG WEI

Department of Cardiology, Shanghai Jiao Tong University Affiliated Sixth People's Hospital, Shanghai 200233, P.R. China

Abstract. Adverse ventricular remodeling is a maladaptive response to acute loss of myocardium and an important risk factor for heart failure following myocardial infarction (MI). Intermedin (IMD) is a novel member of the calcitonin/calcitonin gene-related peptide family, which may possess potent cardioprotective properties. The aim of the present study was to determine whether IMD$_{1\text{-}53}$, a mature bioactive form of IMD, may promote therapeutic angiogenesis within the infarcted myocardium, therefore attenuating adverse ventricular remodeling post-MI. The present study observed that treatment with IMD$_{1\text{-}53}$ promoted proliferation, migration and tube formation of primary cultured myocardial microvascular endothelial cells (MMVECs). In a rat model of MI, chronic administration of IMD$_{1\text{-}53}$ increased capillary density in the peri-infarct zone, attenuated ventricular remodeling and improved cardiac performance post-MI. Treatment with IMD$_{1\text{-}53}$ also significantly increased the expression levels of phosphorylated-AMP-activated protein kinase (AMPK) and the subsequent activation of endothelial nitric oxide synthase in MMVECs and post-MI rat myocardium, without a significant influence on the expression of vascular endothelial growth factor. Notably, the *in vitro* effects of IMD$_{1\text{-}53}$ on angiogenesis and the *in vivo* effects of IMD$_{1\text{-}53}$ on post-MI ventricular remodeling were largely abrogated by the co-administration of compound C, an AMPK inhibitor. In conclusion, the present study demonstrated that IMD$_{1\text{-}53}$ could attenuate adverse ventricular remodeling post-MI via the promotion of therapeutic angiogenesis, possibly through the activation of AMPK signaling.

Correspondence to: Professor Meng Wei, Department of Cardiology, Shanghai Jiao Tong University Affiliated Sixth People's Hospital, 600 Yishan Road, Shanghai 200233, P.R. China
E-mail: wmsjtu6h@163.com

[*]Contributed equally

Introduction

Ventricular remodeling, which is characterized by progressive dilation and deterioration in cardiac performance, is a critical process underlying the progression to heart failure and subsequent mortality following myocardial infarction (MI). As a result, the attenuation of adverse myocardial remodeling is one of the most important aspects for improving prognosis following MI (1). However, despite previous advances in reperfusion therapy and optimized pharmacological treatments, left ventricular (LV) remodeling is still observed in a substantial proportion of patients, and progression to heart failure can still occur in up to one-third of patients who have had a MI (2,3). These data suggest that the current clinical treatments targeting myocardial remodeling post-MI remain inadequate. The promotion of therapeutic angiogenesis has been demonstrated to be a promising approach to ameliorate adverse myocardial remodeling (4).

Intermedin (IMD), also known as adrenomedullin 2, is a novel member of the calcitonin/calcitonin gene-related peptide (CGRP) family. The human IMD gene encodes a prepropeptide of 148 amino acids (preproIMD); proteolytic cleavage of preproIMD yields a series of biologically active C-terminal fragments. Previous studies have revealed that an endogenous degraded fragment termed IMD$_{1\text{-}53}$, which contains cleavage sites located between two basic amino acids at Arg93-Arg94, possessed potent cardioprotective activities in multiple physiopathological processes, including ischemia/reperfusion injury (5,6), cardiac fibrosis (7) and cardiac hypertrophy (8,9). However, the mechanisms underlying the cardioprotective effects of IMD require further elucidation. Notably, IMD was also reported to serve a role in the regulation of angiogenesis *in vitro* and *in vivo* (10,11). However, whether IMD$_{1\text{-}53}$ may promote therapeutic angiogenesis within the infarcted myocardium, and therefore attenuate adverse myocardial remodeling post-MI, has not been investigated. To test this hypothesis, the present study investigated the effects of recombinant IMD$_{1\text{-}53}$

on angiogenesis in primary cultured myocardial microvascular endothelial cells (MMVECs) and in a rat model of MI. The results suggested that IMD_{1-53} attenuated adverse ventricular remodeling post-MI by promoting therapeutic angiogenesis, possibly through the activation of AMP-activated protein kinase (AMPK) signaling.

Materials and methods

Materials. IMD_{1-53} peptide was purchased from Phoenix Pharmaceuticals, Inc. (Burlingame, CA, USA). Dulbecco's modified Eagle's medium (DMEM) and fetal bovine serum (FBS) were purchased from Gibco (Thermo Fisher Scientific, Inc., Waltham, MA USA). Phosphorylated (p)-AMPK$\alpha^{Thr-172}$ (cat. no. 2535), AMPKα (cat. no. 2532), p-Akt$^{Ser-473}$ (cat. no. 4060), and p-endothelial nitric oxide synthase (p-eNOS)$^{Ser-1179}$ (cat. no. 9570) antibodies were purchased from Cell Signaling Technology, Inc. (Danvers, MA, USA). Anti-Akt (cat. no. sc-8312), anti-eNOS (cat. no. sc-654), anti-GAPDH (cat. no. sc-25778) and anti-VEGF (cat. no. sc-152), anti-CD31 (cat. no. sc-1505) anti-CD34 (cat. no. sc-7045) antibodies were purchased from Santa Cruz Biotechnology, Inc. (Dallas, TX, USA). Compound C (Comp C) was purchased from Toronto Research Chemicals Inc. (North York, ON, Canada). Goat anti-rabbit (cat. no. sc-2030) and goat anti-mouse (cat. no. sc-3791) secondary antibodies were purchased from Santa Cruz Biotechnology, Inc.

For all experiments concerning IMD_{1-53}, the same volume of PBS was used as a vehicle. For experiments concerning Comp C, the same volume of DMSO was used as a vehicle.

Isolation and identification of MMVECs. Male Wistar rats (n=16; 4-6 weeks; 80-100 g) were used for the isolation of primary MMVECs. The rats were housed at room temperature with a 12/12 h light/dark cycle and free access to food and water. The animal protocol was approved by the Animal Care Committee of Shanghai Jiao Tong University (Shanghai, China). Rats were sacrificed with an overdose of sodium pentobarbital (180 mg/kg) and heparinized by intraperitoneal injection of sodium heparin (500 units/0.1 kg). Following thoracotomy, the heart was rapidly dislodged and washed in PBS. The atria, right ventricle, epicardial tissue and visible connective tissue were carefully removed, and the remaining myocardial tissue was washed in PBS prior to cutting into $1 mm^3$ sections without visible vessels. Myocardial tissues were seeded onto culture plates that were pre-coated with rat tail tendon gelatin and subsequently incubated at 37°C in a humidified atmosphere containing 5% CO_2 for 30 min. Tissues were cultured in DMEM containing 4,500 mg/l D-glucose and supplemented with 20% FBS, 50 U/ml heparin, 100 U/ml penicillin and 100 μg/ml streptomycin. Tissue sections were discarded after the cells began to grow, and the medium was replaced at 72 h intervals. MMVECs were identified by typical 'cobblestone' appearance and positive CD31 and CD34 immunostaining. MMVECs at the second passage were used for experiments. The cells were grown to 80-90% confluence and were used in subsequent experimental analyses.

Immunostaining. MMVECs were plated on a 12x12 mm plate, fixed by methanol for 15 min at -20°C, blocked with 10% normal goat serum (cat. no. 31872; Gibco; Thermo Fisher Scientific, Inc.) for 30 min at room temperature, incubated with CD31 (cat. no. sc-1505; Santa Cruz Biotechnology, Inc.) and CD34 (cat. no. sc-7045; Santa Cruz Biotechnology, Inc.) antibodies at 1:200 overnight at 4°C, and then incubated with goat anti-mouse secondary antibody (cat. no. sc-3791; Santa Cruz Biotechnology, Inc.) at 1:1,500 for 1 h at room temperature. Finally, DAB working solution diluted by H_2O_2 was added and the MMVECs were observed under a light microscope (Olympus IX71; Olympus Corporation, Tokyo, Japan).

Cell proliferation assay. The proliferation rate of MMVECs was assessed using the MTT assay (Sigma-Aldrich; Merck Millipore, Darmstadt, Germany). The cells were seeded into 96-well plates at a density of $2x10^3$ cells/well and incubated in DMEM containing 10% FBS at 37°C with 5% CO_2 for 24 h. IMD_{1-53}, Comp C or IMD_{1-53}+Comp C was added to the medium at different concentrations (0, 10, 20, 40, 80, 160 nm of IMD and/or 20 μmol compound C) at 0 h. Following 0, 8, 16, 24 and 48 h incubation, 10 μl of MTT was added to each well and the cells were incubated at 37°C for 4 h. Following incubation, the supernatant fluid was removed and 100 μl dimethyl sulfoxide was added to each well. The cells were incubated for 10 min and the absorbance at 490 nm was measured with an Epoch Microplate Spectrophotometer (BioTek Instruments, Inc., Winooski, VT, USA).

Migration assay. MMVEC migration rate was assessed using the Boyden Chemotaxis Chamber assay (Neuro Probe, Inc., Gaithersburg, MD, USA). The cells were trypsinized and resuspended in 10% DMEM containing 10% FBS. IMD_{1-53} (80 nmol) and/or Comp C (20 μmol) were added to the wells in the lower chamber, and $1.5x10^4$ cells (200 μl/well) were added into the upper chamber. Cells migrating through the filter were fixed in 4% paraformaldehyde for 10 min and subsequently stained with 0.1% crystal violet stain solution (Merck Millipore) for 30 min. Five random microscopic fields per well were quantified using an Olympus IX71 fluorescence microscope (Olympus Corporation). Each experiment was repeated three times.

Tube formation assay. Tube formation of MMVECs was assessed using a Matrigel assay (BD Biosciences, Franklin Lakes, NJ, USA). Matrigel was chilled at 4°C overnight, melted prior to use and then quickly added (70 μl/well) to 96-well plates using a pre-chilled pipette. The plates were incubated at 37°C in 5% CO_2 for 1 h. The cells were seeded into the plates at a density of $1x10^4$ cells/well and incubated for 12 h in the presence or absence of IMD_{1-53} (80 nmol) and/or Comp C (20 μmol) at 37°C. Tube formation was observed and images were captured using an Olympus 1X71 microscope (Olympus Corporation). Images were processed using Image-Pro Plus software 6.0 (Media Cybernetics, Inc., Rockville, MD, USA) to calculate the degree of tube formation by measuring the length of tubes from five randomly selected fields (magnification, x200) from each well. Each experiment was repeated three times.

Western blot analysis. Cell or tissue samples were homogenized as follows: Freshly frozen myocardial tissue samples were ground into small pieces (~1x1x1 mm) in liquid nitrogen

with a mortar and a pestle. The samples were transferred to microcentrifuges containing radioimmunoprecipitation lysis buffer (~150 μl per 10 mg tissue; Beyotime Institute of Biotechnology, Haimen, China) and 1 mM phenylmethyl-sulfonyl fluoride. The samples were then kept on ice for 1 h, vortexing every 10 min. The lysates were then centrifuged at 10,000 x g for 30 min at 4°C, and supernatants were removed for immediate western blot analysis. Protein samples (5 mg/ml) were loaded onto a 10% Bis-Tris gel; following electrophoresis, separated proteins were transferred to a polyvinylidene fluoride membrane for 1 h. The membranes were then incubated with blocking solution (5% skim milk) for 1-2 h at room temperature, followed by three washes with TBS-Tween-20 (TBST; 0.1% Tween; 10 min each). Membranes were incubated with one of the following primary antibodies: Anti-AMPK (1:800); anti-p-AMPK^{Thr172} (1:1,000); anti-Akt (1:1,500); anti-p-Akt^{ser473} (1:1,000); anti-eNOS (1:500); anti-p-eNOS^{ser1117} (1:500); anti-vascular endothelial growth factor (VEGF; 1:1,000); and anti-GAPDH (1:8,000) at 4°C overnight. Primary antibodies were recovered and the membranes were washed three times with TBST (10 min each), followed by incubation with horse-radish peroxidase-conjugated goat anti-rabbit immunoglobulin G (IgG; cat. no. sc-2030; 1:2,000) secondary antibody at room temperature for 1 h. Subsequently, the membranes were washed five times with TBST (5 min/wash), and the bands were detected using Western Blotting Luminol Reagent (Santa Cruz Biotechnology, Inc.) and quantified by densitometric analysis of digitized autoradiograms using Quantity One (version 4.6.2) software (Bio-Rad Laboratories, Inc., Hercules, CA, USA). Each immunoblotting experiment was repeated three times, and the averages of the results were calculated.

Animal model. A total of 70 male Sprague-Dawley rats (age, 8 weeks; weight, 250-280 g; Experimental Animal Center, Fudan University, Shanghai, China) were used in the present study, and were maintained at room temperature with a 12/12 h light/dark cycle and free access to food and water. The animal research study protocol was in compliance with the Guide for the Care and Use of Laboratory Animals published by the National Institutes of Health (NIH Publication no. 85-23, revised 1996) and approved by the Animal Care Committee of Shanghai Sixth Hospital, Shanghai Jiao Tong University. All rats were acclimated for 2 weeks prior to experimentation. All rats were anesthetized by intraperitoneal injection of pentobarbital sodium (60 mg/kg) and ventilated using a DW-200 animal respirator (Shanghai Alcott Biotech Co., Ltd., Shanghai, China) with room air following endotracheal intubation. Electrocardiogram (ECG) lead II was continuously monitored during the experiment. Heart exposure was performed by a thoracotomy at the left fourth intercostal space. The left anterior descending (LAD) coronary artery was ligated using a size 6-0 Prolene polypropylene suture, 1-2 mm below the tip of the left atrial appendage. LAD ligation was confirmed by a color change of the myocardium and an elevation of the ST segment on the ECG. A total of 4 weeks after LAD ligation, all the surviving rats were sacrificed by injection of 180 mg/kg pentobarbital sodium overdose.

Animal protocols. A total of 70 Sprague-Dawley rats were randomly divided and assigned to five treatment groups: i) Sham group (n=10), which underwent thoracotomy and incision of the pericardial sac without LAD ligation; ii) MI group (n=15), which underwent LAD ligation without any treatment; iii) IMD group (n=15), which contained MI rats that received subsequent intraperitoneal injections of IMD$_{1-53}$ (10 nmol/kg/day) starting 3 days after LAD ligation; iv) IMD+Comp C group (n=15), which contained MI rats that received subsequent intraperitoneal injections of IMD$_{1-53}$ (10 nmol/kg/day) and Comp C (5 mg/kg/day) starting 3 days after LAD ligation; and v) Comp C group (n=15), which contained MI rats that received subsequent intraperitoneal injections of Comp C (5 mg/kg) starting 3 days after LAD ligation.

Echocardiography. An echocardiographic examination was performed on day 28 following the induction of MI using a standard Acuson Sequoia 512 ultrasound system equipped with a 15 MHz probe (Siemens AG, Munich, Germany). Two-dimensional and motion-mode echocardiography were performed. The LV end-diastolic diameter (LVEDD) and the LV end-systolic diameter (LVESD) were measured. In addition, the LV ejection fraction (LVEF) and fractional shortening (FS) were calculated as previously described (12). All measurements from five consecutive cardiac cycles were averaged and analyzed by a single observer that was blinded to the treatment protocol.

Histological analysis. Under deep anesthesia with pentobarbital sodium (intraperitoneal injection at 100 mg/kg), the heart was excised and cut into 2-mm-thick transverse slices, which were then fixed in 10% formalin solution at room temperature for 24 h. The samples were subsequently embedded in paraffin and sectioned (4 μm). Immunohistochemical analysis was performed as previously described (13). Tissue sections were then depa-raffinized using xylene and graded ethanol and were blocked in 10% goat serum (Gibco, Thermo Fisher Scientific, Inc.) for 30 min at 37°C. Samples were incubated at 4°C overnight with primary rabbit polyclonal antibodies against CD31 (ab28364) and VEGF (ab46154; Abcam, Cambridge). Sections were subsequently treated with secondary goat polyclonal secondary antibody against rabbit IgG (ab97047; Abcam). All sections were counterstained with hematoxylin. Immunoreactivity for CD31 and VEGF was measured using a fluorescence microscope and the Image-Pro Plus 4.0 analysis system (Media Cybernetics, Inc.). Capillaries were identified by positive staining for CD31. Results were expressed as the average amount of capillaries per x10 field. Masson's trichrome stain was performed in the border area to evaluate collagen deposition.

Statistical analysis. Statistical analysis of the data was conducted using the statistical software SPSS version 13.0 (SPSS, Inc., Chicago, IL, USA). Experimental data were expressed as the mean ± standard deviation and analyzed using one-way ANOVA followed by a least-significant difference corrected multiple comparison test. $P<0.05$ was considered to indicate a statistically significant difference.

Results

IMD$_{1-53}$ increases proliferation of MMVECs in a dose-dependent manner. The effects of IMD$_{1-53}$ on the

proliferation of MMVECs were examined using the MTT assay. The results indicated that IMD$_{1\text{-}53}$ was able to promote the proliferation of MMVECs in a dose-dependent manner with the maximum effect observed at 80 nmol (P<0.05 vs. 0 nmol control, Fig. 1A). In addition, co-administration of Comp C, a well-known inhibitor of AMPK, significantly attenuated the effects of IMD$_{1\text{-}53}$ on the proliferation of MMVECs (P<0.05 vs. IMD at 8, 16, 24 and 48 h; Fig. 1B), whereas treatment with Comp C alone had no significant influence on the proliferation of MMVECs (P>0.05, Fig. 1B).

IMD$_{1\text{-}53}$ promotes migration and tube formation in MMVECs. The effects of IMD$_{1\text{-}53}$ on endothelial cell migration were further evaluated by a modified Boyden chamber assay (Fig. 2). The results indicated that the optimal dose (80 nmol, as shown in the MTT assay) of IMD$_{1\text{-}53}$ treatment stimulated the migration of MMVECs (P<0.05 vs. control, Fig. 2A and C). Co-treatment with Comp C (20 μmol) partially suppressed the pro-migratory effect of IMD$_{1\text{-}53}$ (P<0.05 vs. IMD, Fig. 2A and C).

To examine the effects of IMD$_{1\text{-}53}$ on the differentiation of cardiovascular endothelial cells into vascular structures, MMVECs were plated at 1×10^4 cells/well in the presence or absence of IMD$_{1\text{-}53}$ (80 nmol) and/or Comp C (20 μmol) and tube formation was detected microscopically. A total of 24 h after plating, the MMVECs treated with IMD$_{1\text{-}53}$ formed a significantly more extensive tube network compared with the control group (P<0.05). The effects of IMD$_{1\text{-}53}$ on tube formation were reduced in MMVECs that were also pretreated with Comp C (P<0.05 vs. IMD group). Treatment with Comp C alone significantly decreased tube formation as compared with the control group (P<0.05, Fig. 2B and D).

IMD$_{1\text{-}53}$ stimulates activation of the AMPK-Akt-eNOS signaling pathway in MMVECs. Since AMPK is involved in the regulation of angiogenesis (14) and IMD$_{1\text{-}53}$ was recently reported to increase AMPK activation in rat cardiomyocytes (9), the present study aimed to investigate whether AMPK is involved in IMD$_{1\text{-}53}$-induced angiogenesis in MMVECs. MMVECs were exposed to IMD$_{1\text{-}53}$ (80 nmol) for 2 h; subsequently, the total and phosphorylated protein levels of AMPKα, Akt and eNOS were analyzed by western blot analysis. As shown in Fig. 3, the expression levels of p-AMPKα, p-Akt and p-eNOS were all significantly increased by IMD$_{1\text{-}53}$ treatment (P<0.05 vs. control, Fig. 3). Co-treatment with the Comp C suppressed the ability of IMD$_{1\text{-}53}$ to activate either Akt or eNOS, as measured by the relative expression levels of p-Akt and p-eNOS (P<0.05 vs. IMD, Fig. 3), whereas treatment with Comp C alone slightly but significantly decreased the phosphorylated levels of Akt and eNOS (P<0.05, respectively; Fig. 3) and significantly decreased the phosphorylated levels of AMPKα (P<0.05; Fig. 3).

IMD$_{1\text{-}53}$ increases capillary density in post-MI rat heart. To assess the effects of IMB of angiogenesis *in vivo*, myocardium capillary density tests were performed. Compared with the sham group, induction of MI significantly increased the capillary density in the peri-infarct zone (P<0.05, Fig. 4A and C). Treatment with IMD$_{1\text{-}53}$ significantly increased capillary density in the peri-infarct zone of post-MI rat myocardium (P<0.05 vs. MI, Fig. 4A and C). Co-administration of Comp

C mitigated the effects of IMD$_{1\text{-}53}$ on capillary density in the peri-infarct zone (P<0.05 vs. IMD, Fig. 4A and C). Compared with the MI group, administration of Comp C alone slightly decreased capillary density in the peri-infarct zone (P<0.05, Fig. 4A and C). Compared to the sham group, the expression levels of VEGF were increased following induction of MI (P<0.05, Fig. 4B and D). However, the administration of IMD$_{1\text{-}53}$, Comp C or a combination of the two had no significant effect on VEGF expression in the peri-infarct zone post-MI (P>0.05 vs. MI group, Fig. 4B and D).

IMD$_{1\text{-}53}$ attenuates ventricular remodeling post-MI. To evaluate the effects of IMD$_{1\text{-}53}$ on ventricular remodeling post-MI, Masson's trichrome staining was performed on all groups 4 weeks post-MI induction (Fig. 5). The results demonstrated that treatment with IMD$_{1\text{-}53}$ markedly suppressed elongation of the infarct wall segment and dilation of the LV, as demonstrated by cross-section morphology (Fig. 5A) and calculated by infarct size post-MI (P<0.05 vs. MI group; Fig. 5B). The effects of IMD$_{1\text{-}53}$ on ventricular remodeling were abrogated by co-administration of Comp C (P<0.05 vs. IMD, Fig. 5), whereas Comp C alone had no significant effect on myocardial infarct size post-MI (P>0.05 vs. MI, Fig. 5).

IMD$_{1\text{-}53}$ improves cardiac function post-MI. A total of 4 weeks after MI induction, cardiac geometry and performance were evaluated using echocardiography (Table I). Compared with the sham group, significantly decreased LVEF and FS, along with increased LVESD and LVEDD, were observed in the MI group (P<0.05, Table I). In IMD-treated MI rats, LVEF and FS were significantly improved, whereas LVESD and LVEDD were significantly reduced, compared with the MI group (P<0.05, Table I). Co-administration of Comp C abrogated the effects of IMD$_{1\text{-}53}$ on LVEF, FS, LVESD and LVEDD (P<0.05 vs. IMD, Table I), whereas Comp C alone had no significant effects on cardiac geometry and performance (P>0.05, Table I). Neither IMD$_{1\text{-}53}$ nor Comp C administration had significant effects on survival rate of rats post-MI (P>0.05 vs. MI group; Table I).

IMD$_{1\text{-}53}$ stimulates activation of the AMPK-Akt-eNOS signaling pathway in post-MI rat myocardium. Western blot analysis was used to evaluate the activation of AMPK, Akt and eNOS, and the expression levels of VEGF in rat myocardium (Fig. 6). The results indicated that chronic IMD$_{1\text{-}53}$ treatment resulted in significantly increased activation (as measured by phosphorylation) of AMPK, Akt and eNOS in post-MI rat myocardium (P<0.05 vs. MI, Fig. 6B-D), whereas it had no significant effect on the expression of VEGF (P>0.05 vs. MI, Fig. 6A). Co-administration of Comp C abrogated the effects of IMD$_{1\text{-}53}$ on AMPK, Akt and eNOS phosphorylation (P<0.05 vs. IMD, Fig. 6B-D), whereas Comp C alone slightly decreased levels of p-AMPK, p-Akt and p-eNOS (P<0.05 vs. MI, Fig. 6B-D).

Discussion

Using *in vitro* and *in vivo* experiments, the present study demonstrated that IMD$_{1\text{-}53}$ promoted angiogenesis in primary cultured MMVECs, which was demonstrated by an increase
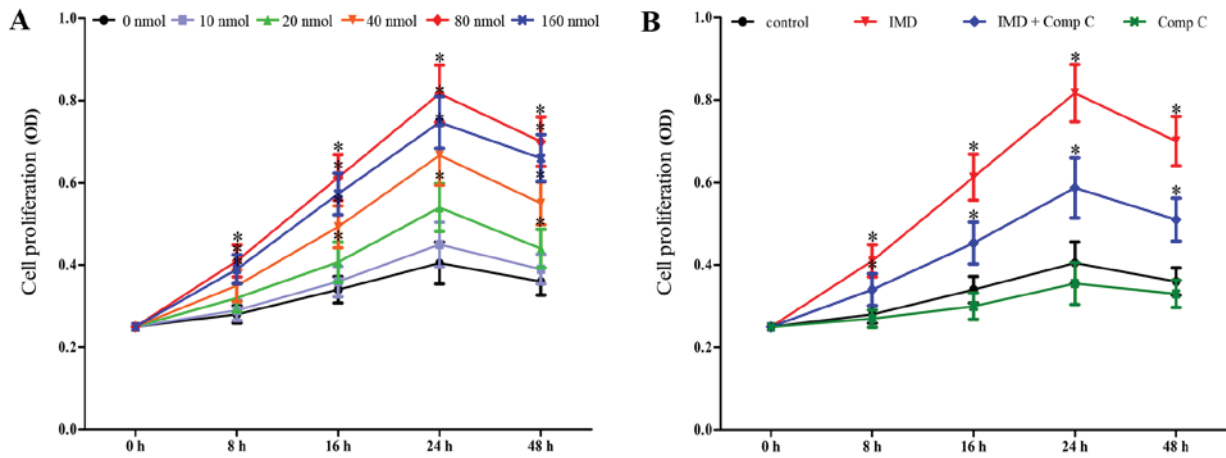
Figure 1. IMD$_{1-53}$ promotes the proliferation of MMVECs. Proliferation was assessed using the MTT assay. (A) MMVECs were seeded in 96-well dishes in the presence of different concentrations (0-160 nmol) of IMD$_{1-53}$ for 0, 8, 16, 24 and 48 h. (B) MMVECs were seeded in 96-well dishes in the presence of IMD$_{1-53}$ (80 nmol), Comp C (20 μmol), or both for 0, 8, 16, 24 and 48 h. All data are expressed as the mean ± standard deviation from three independent experiments. *P<0.05 vs. control group. Comp C, compound C; IMD, intermedin; MMVECs, myocardial microvascular endothelial cells.
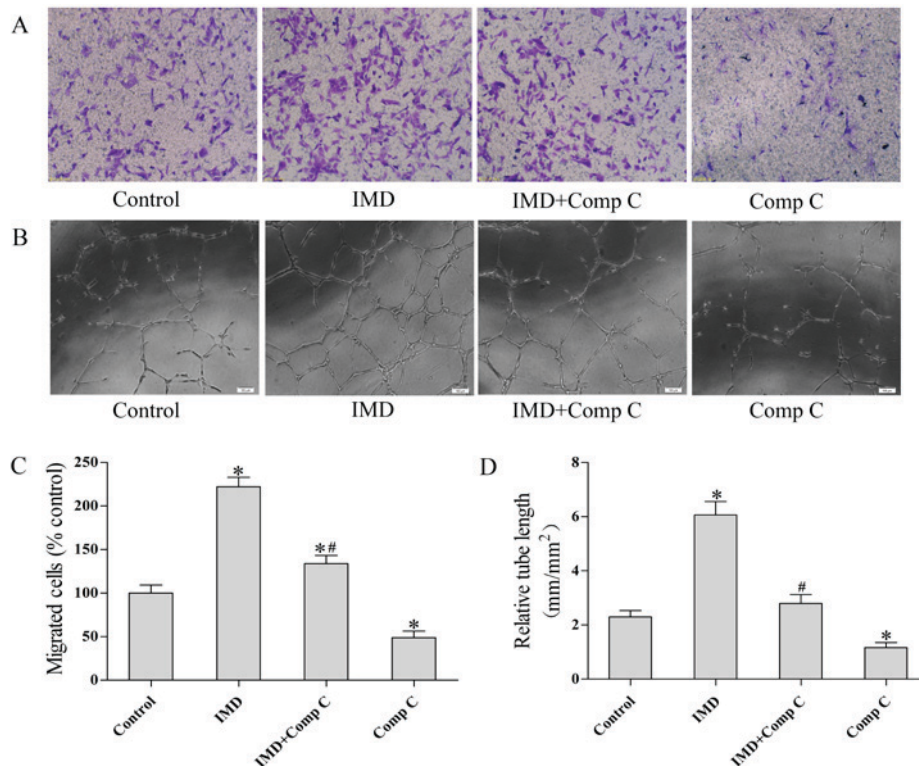

Figure 2. IMD$_{1-53}$ promotes the migration of MMVECs and their differentiation into tube-like structures. (A) Representative images of the migration of MMVECs assessed by Boyden chamber analysis. Magnification, x100. (B) Representative images of *in vitro* tube formation analysis of MMVECs on Matrigel. Magnification, x200. Quantitative analysis of the (C) migration and (D) tube formation assays. Each treatment was performed in triplicate and five fields were randomly selected from each well for counting the number of migrated cells. All data are expressed as the mean ± standard deviation. *P<0.05 vs. control; #P<0.05 vs. IMD group. Comp C, compound C; IMD, intermedin; MMVECs, myocardial microvascular endothelial cells.

in proliferation, migration and tube formation. In addition, experiments using an *in vivo* rat model of MI demonstrated that treatment with IMD$_{1-53}$ significantly increased the capillary density in ischemic myocardium, attenuated LV remodeling and improved post-MI cardiac function, as determined by CD31 staining, Masson trichrome staining and echocardiography, respectively. Furthermore, the addition of Comp C, an AMPK inhibitor, demonstrated that the *in vitro* and the

in vivo effects of IMD$_{1-53}$ were at least partially dependent on the activation of AMPK. These results indicated that IMD$_{1-53}$ attenuates post-infarct myocardial remodeling via the promotion of AMPK-dependent angiogenesis. To the best of our knowledge, this is the first demonstration of the involvement of AMPK activation in IMD-induced angiogenesis and is one of only a few studies (8,10,15) to link the cardioprotective role of IMD to therapeutic angiogenesis.
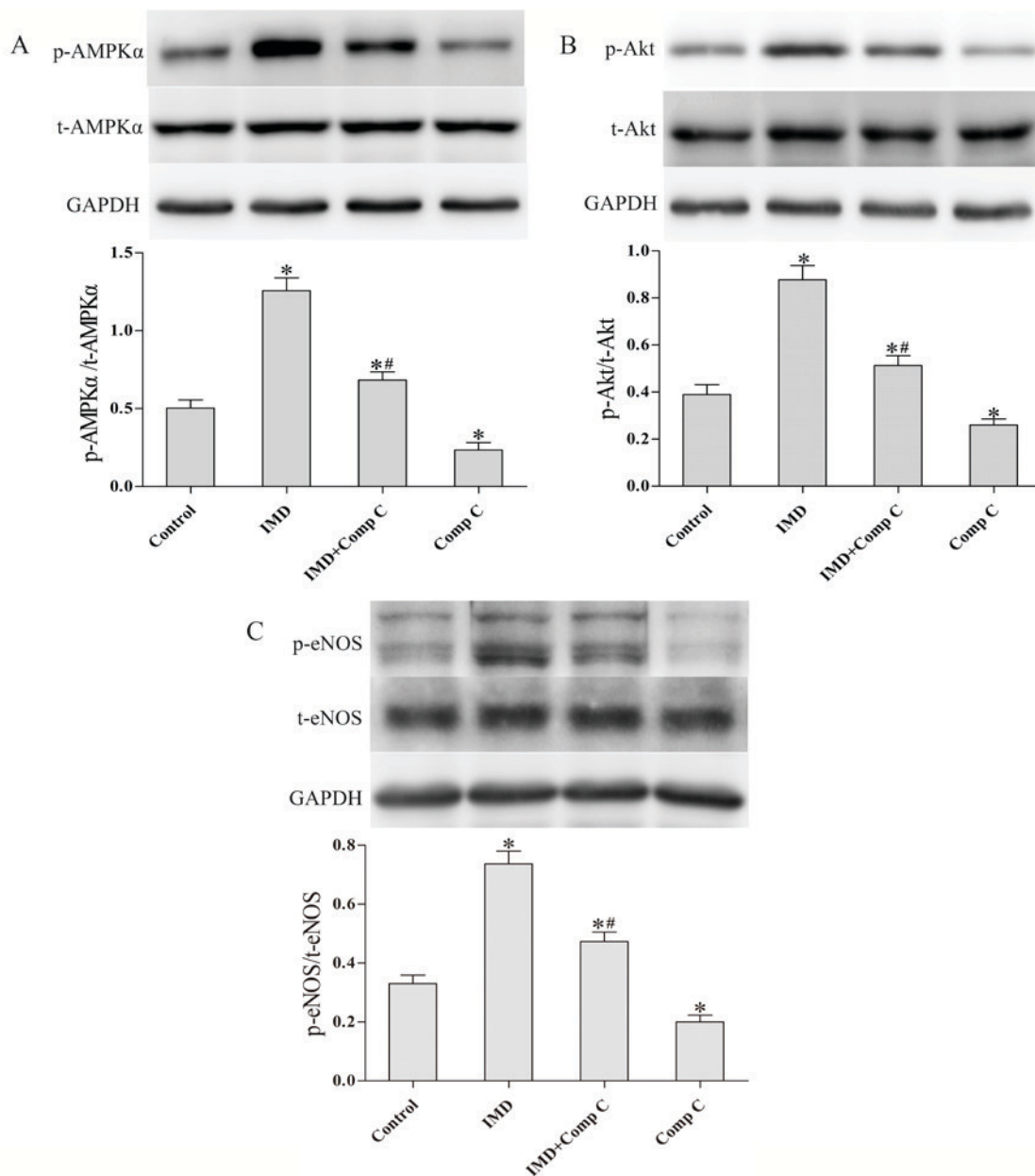
Figure 3. Effects of IMD$_{1-53}$ on the level of expression and phosphorylation of AMPKα, Akt and eNOS in MMVECs. MMVECs were pretreated with either Comp C (20 μmol) or vehicle for 40 min and incubated with either IMD$_{1-53}$ (80 nmol) or vehicle for 2 h prior to harvest. Representative western blots demonstrating (A) p-AMPKα over total AMPKα protein expression, (B) p-Akt over total Akt protein expression and (C) p-eNOS over total eNOS protein expression. All data are expressed as the mean ± standard deviation; *P<0.05 vs. control group; #P<0.05 vs. IMD group. AMPKα, AMP-activated protein kinase α; Comp -C, compound C; eNOS, endothelial nitric oxide synthase; IMD, intermedin; MMVECs, myocardial microvascular endothelial cells; p, phosphorylated.

The human IMD gene encodes a prepropeptide of 148 amino acids (preproIMD), which can generate a series of mature peptide fragments by proteolytic cleavage at the C-terminal *in vivo* (16), such as IMD$_{1-47}$, IMD$_{8-47}$ and IMD$_{1-53}$. Yang *et al* were the first to report that IMD$_{1-53}$ stimulated L-Arg transport and increased NOS activity in the rat aorta (15). Furthermore, using direct gene delivery, Smith *et al* established IMD as a novel angiogenic factor in a rodent hindlimb ischemia model and cultured human umbilical vein endothelial cells (10). Consistent with these findings, the present study demonstrated that IMD$_{1-53}$ increased proliferation of MMVECs in a dose-dependent manner with a maximal effect at around 80 nmol, and the optimal dose of IMD$_{1-53}$ treatment promoted migration and tube formation of MMVECs.

Cardiac hypertrophy is initiated as an adaptive response during post-infarction remodeling to compensate for increased load (17). However, the capillary network within the infarcted heart is unable to support the increased demands of the hypertrophied myocardium, resulting in a gradual loss of healthy tissue, extension of the infarct and fibrous replacement (18). Therefore, promotion of angiogenesis in post-infarct myocardium may be an effective approach to attenuate adverse ventricular remodeling following MI, as demonstrated by several previous studies (19-21). The present study demonstrated that the *in vivo* administration of IMD$_{1-53}$ promoted angiogenesis in post-infarct rat myocardium, which was indicated by increased capillary density in the peri-infarct zone. In addition, chronic treatment with IMD$_{1-53}$ preserved
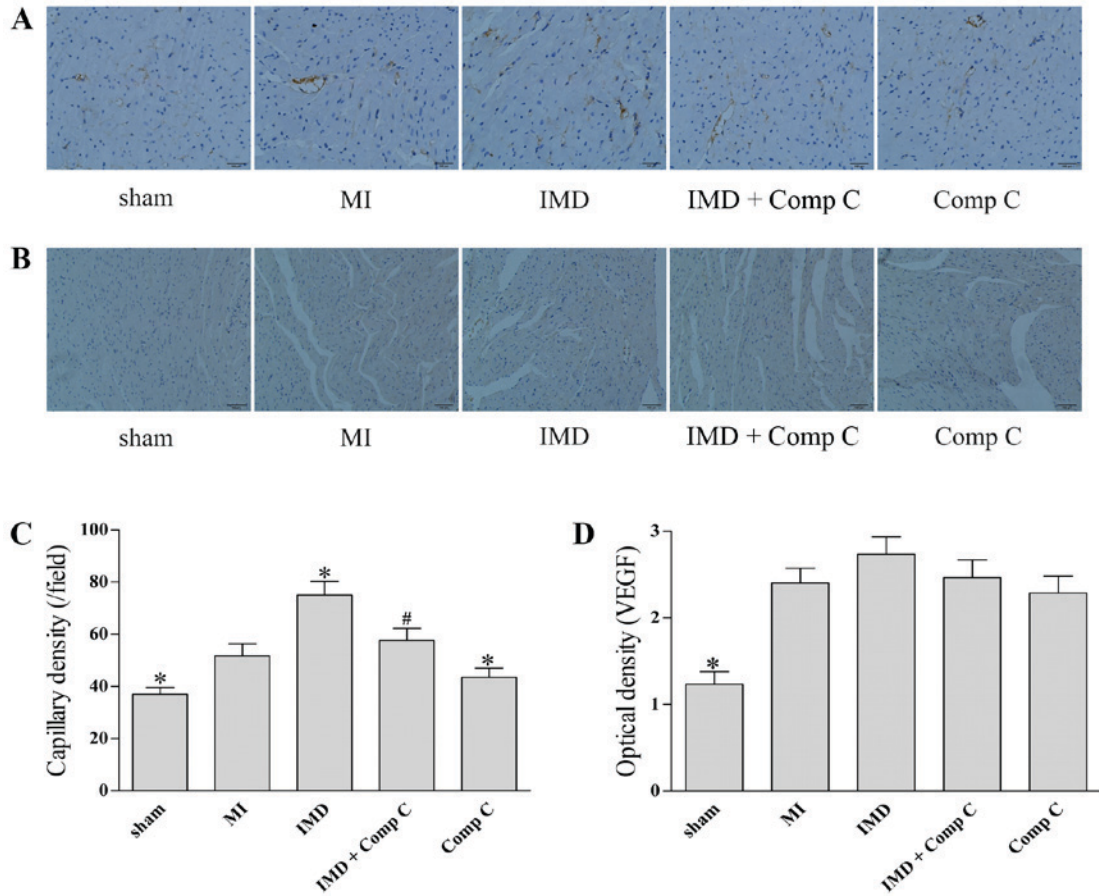
Figure 4. IMD$_{1-53}$ increases capillary density in post-infarct myocardium. Immunohistochemical staining for CD31 and VEGF were performed in each group 4 weeks post-MI induction. Representative slides of tissue from peri-infarct myocardium with (A) CD31 expression and (B) VEGF expression; magnification, x200. Quantification of (C) CD31 (expressed as the number of capillaries per 10x field) and (D) VEGF expression in each group. All data are expressed as the mean ± standard deviation. n=4 for sham group, n=6 for other groups. *P<0.05 vs. MI group; #P<0.05 vs. IMD group. Comp C, Compound C; IMD, intermedin; MI, myocardial infarction; VEGF, vascular endothelial growth factor.
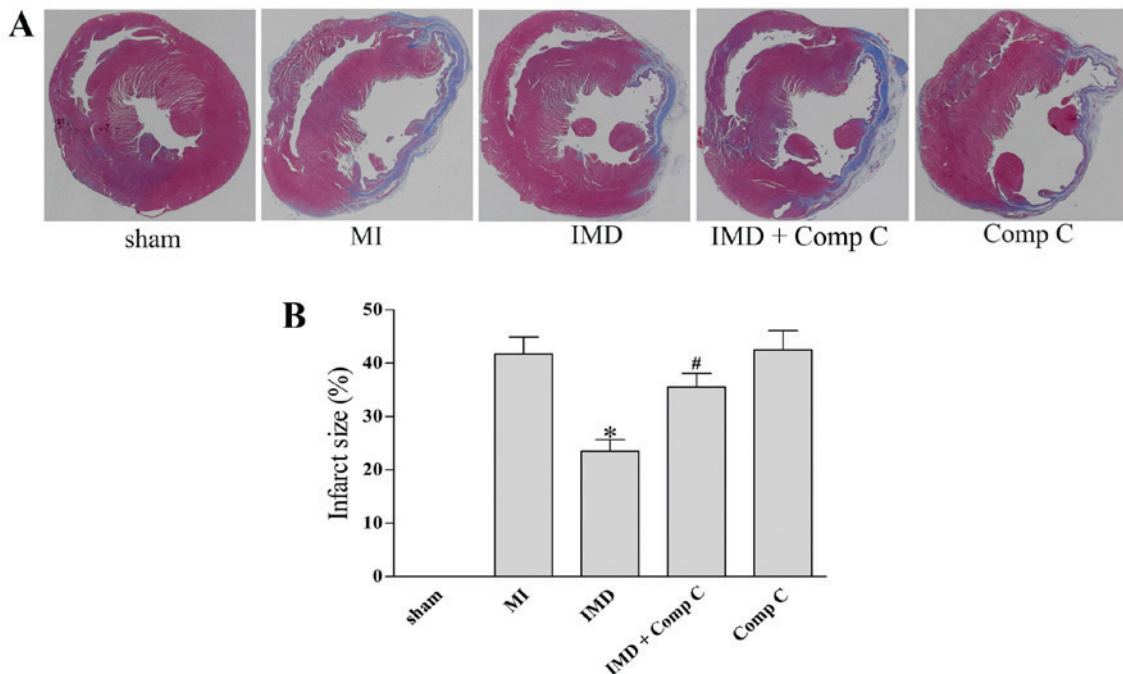

Figure 5. IMD$_{1-53}$ attenuates ventricular remodeling post-MI. (A) Representative Masson's trichrome-stained LV cross-sections obtained 4 weeks post-MI induction from each group; demonstrating the effects of IMD$_{1-53}$ on LV morphology. Fibrotic areas are stained blue and viable myocardium is stained red (x10 magnification). (B) Quantitative assessment of infarct size. Data are expressed as the mean ± standard deviation; n=4 for sham group, n=6 for other groups. *P<0.05 vs. MI group; #P<0.05 vs. IMD group. Comp C, compound C; IMD, intermedin; LV, left ventricle; MI, myocardial infarction.

Table I. Representative motion-mode echocardiograms obtained 4 weeks post-MI induction.

Parameter	Sham	MI	IMD	IMD+Comp C	Comp C
Number	10	15	15	15	15
Survival	10	11	12	11	10
LVESD (mm)	3.47±0.28[a]	6.11±0.31	4.52±0.27[a]	5.84±0.33[b]	6.24±0.28
LVEDD (mm)	5.83±0.36[a]	8.28±0.44	6.42±0.42[a]	7.61±0.49[b]	8.48±0.47
LVEF (%)	81.3±5.38[a]	46.8±5.14	65.2±6.03[a]	53.7±5.93[b]	44.9±5.26
FS (%)	75.6±4.97[a]	44.9±3.71	66.5±4.89[a]	52.2±3.87[b]	43.7±3.54

Summary data of echocardiographic measurements in each group of animals. Data are expressed as the mean ± standard deviation. [a]$P<0.05$ vs. MI group; [b]$P<0.05$ vs. IMD-treated group. Comp C, compound C; FS, fractional shortening; IMD, intermedin; LVEDD, left ventricular end-diastolic diameter; LVEF, left ventricular ejection fraction; LVESD, left ventricular end-systolic diameter; MI, myocardial infarction.
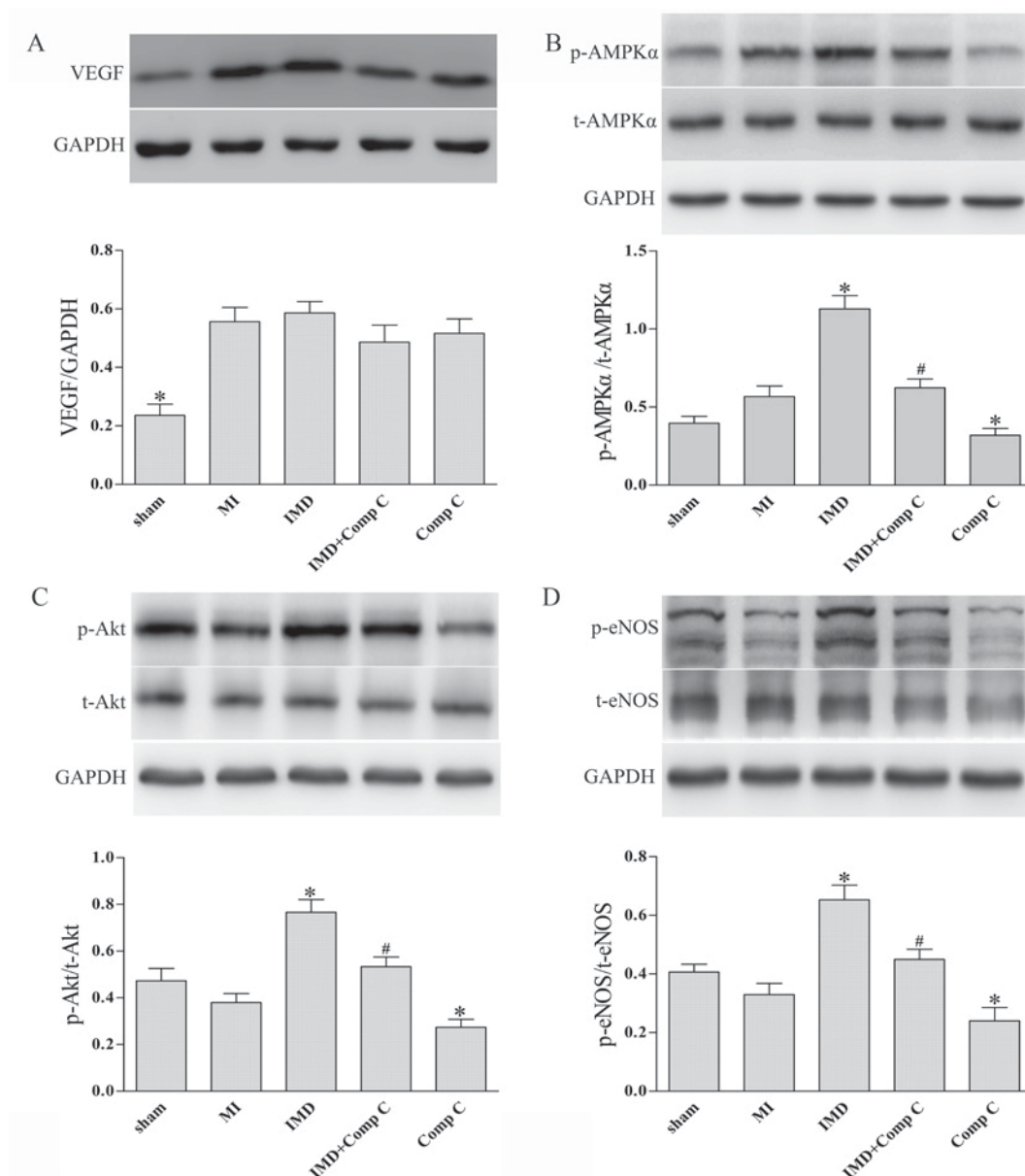

Figure 6. Effects of IMD₁₋₅₃ on expression and phosphorylation of VEGF, AMPK, Akt and eNOS in rat myocardium post-MI. The infarcted heart tissue from the LV free wall or the non-infarcted heart tissue at the same site was harvested 4 weeks after left anterior descending coronary artery ligation. Representative western blots demonstrating (A) VEGF protein expression, GAPDH is used as a loading control; (B) p-AMPK over total AMPK protein expression; (C) p-Akt over total Akt protein expression; and (D) p-eNOS over total eNOS protein expression. Data are expressed as the mean ± standard deviation; n=4 for sham group, n=6 for other groups. *$P<0.05$ vs. MI group; #$P<0.05$ vs. IMD group. AMPK, AMP-activated protein kinase; Comp C, compound C; eNOS, endothelial nitric oxide synthase; IMD, intermedin; MI, myocardial infarction; LV, left ventricle; p, phosphorylated; VEGF, vascular endothelial growth factor.

cardiac geometry and improved cardiac performance post-MI, as evidenced by Masson trichrome staining and echocardiography, suggesting that IMD$_{1-53}$ may attenuate adverse remodeling post-MI and prevent subsequent heart failure by promoting angiogenesis. IMD$_{1-53}$ has previously been reported to protect against myocardial ischemia/reperfusion injury (5) and to attenuate pressure-overload-induced cardiac hypertrophy (9) through other mechanisms (6,8); however, to the best of our knowledge, this is the first study to link the cardioprotective role of IMD to therapeutic angiogenesis.

AMPK is a key sensor and regulator of cellular energy homeostasis, which modulates various physiological processes that may favor the restoration of energy balance in several systems (22). In endothelial cells, AMPK was demonstrated to serve an essential role in angiogenesis in response to stress (14,23). In addition, a series of agents, including pravastatin, adiponectin and erythropoietin, and cytokines have been reported to increase angiogenesis through AMPK-dependent mechanisms (24-26). Notably, CGRP was also reported to promote angiogenesis by activating the AMPK-eNOS pathway in endothelial cells (27). The present study demonstrated that treatment with IMD$_{1-53}$ increased the expression levels of p-AMPK in cultured MMVECs and in post-MI rat myocardium, and notably, administration of Comp C, a known inhibitor of AMPK, abrogated the effects of IMD$_{1-53}$ on angiogenesis, as evidenced by reduced migration and tube formation of MMVECs *in vitro*, and lower capillary density at the peri-infarct zone *in vivo*. These results demonstrated that the angiogenic activity of IMD$_{1-53}$ is at least partially dependent on the activation of AMPK.

It has previously been reported that IMD$_{1-53}$ increased total NOS activity, but had little effect on mRNA levels of either inducible NOS or eNOS in the rat aorta (16). The results of the current study demonstrated that IMD$_{1-53}$ promoted the activation of eNOS *in vitro* and *in vivo*. In addition, the administration of Comp C significantly attenuated the effects of IMD$_{1-53}$ on the level of p-eNOS expression, suggesting that AMPK is involved in the IMD$_{1-53}$-induced activation of eNOS. It is also worth noting that, in the present study, treatment with IMD$_{1-53}$ had no significant effect on the expression of VEGF in post-infarct rat myocardium, indicating that IMD$_{1-53}$ may promote the activation of eNOS and subsequent angiogenesis through VEGF-independent mechanisms. Notably, the present study did not determine how IMD$_{1-53}$ regulated AMPK signaling. In addition, although the α subunit of AMPK was identified as the major target in the present study, further evaluation is required regarding the specific subunit (α1 or α2) involved.

In conclusion, the present study demonstrated that IMD$_{1-53}$ could attenuate adverse ventricular remodeling post-MI by promoting therapeutic angiogenesis, possibly through the activation of AMPK signaling.

Acknowledgements

References

1. Pfeffer MA and Braunwald E: Ventricular remodeling after myocardial infarction. Experimental observations and clinical implications. Circulation 81: 1161-1172, 1990.

2. Jessup M and Brozena S: Heart failure. N Engl J Med 348: 2007-2018, 2003.

3. Mozaffarian D, Benjamin EJ, Go AS, Arnett DK, Blaha MJ, Cushman M, de Ferranti S, Després JP, Fullerton HJ, Howard VJ, *et al*: Heart disease and stroke statistics-2015 update: A report from the American Heart Association. Circulation 131: e29-e322, 2015.

4. Oka T, Akazawa H, Naito AT and Komuro I: Angiogenesis and cardiac hypertrophy: Maintenance of cardiac function and causative roles in heart failure. Circ Res 114: 565-571, 2014.

5. Yang JH, Jia YX, Pan CS, Zhao J, Ouyang M, Yang J, Chang JK, Tang CS and Qi YF: Effects of intermedin(1-53) on cardiac function and ischemia/reperfusion injury in isolated rat hearts. Biochem Biophys Res Commun 327: 713-719, 2005.

6. Zhao L, Peng DQ, Zhang J, Song JQ, Teng X, Yu YR, Tang CS and Qi YF: Extracellular signal-regulated kinase 1/2 activation is involved in intermedin1-53 attenuating myocardial oxidative stress injury induced by ischemia/reperfusion. Peptides 33: 329-335, 2012.

7. Yang X, Zhang H, Jia Y, Ni L, Li G, Xue L and Jiang Y: Effects of intermedin1-53 on myocardial fibrosis. Acta Biochim Biophys Sin (Shanghai) 45: 141-148, 2013.

8. Chen H, Wang X, Tong M, Wu D, Wu S, Chen J, Wang X, Wang X, Kang Y, Tang H, *et al*: Intermedin suppresses pressure overload cardiac hypertrophy through activation of autophagy. PLoS One 8: e64757, 2013.

9. Lu WW, Zhao L, Zhang JS, Hou YL, Yu YR, Jia MZ, Tang CS and Qi YF: Intermedin1-53 protects against cardiac hypertrophy by inhibiting endoplasmic reticulum stress via activating AMP-activated protein kinase. J Hypertens 33: 1676-1687, 2015.

10. Smith RS Jr, Gao L, Bledsoe G, Chao L and Chao J: Intermedin is a new angiogenic growth factor. Am J Physiol Heart Circ Physiol 297: H1040-H1047, 2009.

11. Zhang W, Wang LJ, Xiao F, Wei Y, Ke W and Xin HB: Intermedin: A novel regulator for vascular remodeling and tumor vessel normalization by regulating vascular endothelial-cadherin and extracellular signal-regulated kinase. Arterioscler Thromb Vasc Biol 32: 2721-2732, 2012.

12. Derumeaux G, Mulder P, Richard V, Chagraoui A, Nafeh C, Bauer F, Henry JP and Thuillez C: Tissue Doppler imaging differentiates physiological from pathological pressure-overload left ventricular hypertrophy in rats. Circulation 105: 1602-1608, 2002.

13. Wang F, Huang D, Zhu W, Li S, Yan M, Wei M and Li J: Selective inhibition of PKCβ2 preserves cardiac function after myocardial infarction and is associated with improved angiogenesis of ischemic myocardium in diabetic rats. Int J Mol Med 32: 1037-1046, 2013.

14. Nagata D, Mogi M and Walsh K: AMP-activated protein kinase (AMPK) signaling in endothelial cells is essential for angiogenesis in response to hypoxic stress. J Biol Chem 278: 31000-31006, 2003.

15. Yang JH, Pan CS, Jia YX, Zhang J, Zhao J, Pang YZ, Yang J, Tang CS and Qi YF: Intermedin1-53 activates L-arginine/nitric oxide synthase/nitric oxide pathway in rat aortas. Biochem Biophys Res Commun 341: 567-572, 2006.

16. Roh J, Chang CL, Bhalla A, Klein C and Hsu SY: Intermedin is a calcitonin/calcitonin gene-related peptide family peptide acting through the calcitonin receptor-like receptor/receptor activity-modifying protein receptor complexes. J Biol Chem 279: 7264-7274, 2004.

17. Sutton MG and Sharpe N: Left ventricular remodeling after myocardial infarction: Pathophysiology and therapy. Circulation 101: 2981-2988, 2000.

18. Kocher AA, Schuster MD, Szabolcs MJ, Takuma S, Burkhoff D, Wang J, Homma S, Edwards NM and Itescu S: Neovascularization of ischemic myocardium by human bone-marrow-derived angioblasts prevents cardiomyocyte apoptosis, reduces remodeling and improves cardiac function. Nat Med 7: 430-436, 2001.

19. Li J, Zhang Y, Li C, Xie J, Liu Y, Zhu W, Zhang X, Jiang S, Liu L and Ding Z: HSPA12B attenuates cardiac dysfunction and remodelling after myocardial infarction through an eNOS-dependent mechanism. Cardiovasc Res 99: 674-684, 2013.

20. Vandoorne K, Vandsburger MH, Raz T, Shalev M, Weisinger K, Biton I, Brumfeld V, Raanan C, Nevo N, Eilam R, *et al*: Chronic Akt1 deficiency attenuates adverse remodeling and enhances angiogenesis after myocardial infarction. Circ Cardiovasc Imaging 6: 992-1000, 2013.

21. Zhao X, Balaji P, Pachon R, Beniamen DM, Vatner DE, Graham RM and Vatner SF: Overexpression of cardiomyocyte α1A-Adrenergic receptors attenuates postinfarct remodeling by inducing angiogenesis through heterocellular signaling. Arterioscler Thromb Vasc Biol 35: 2451-2459, 2015.

22. Grahame Hardie D: AMP-activated protein kinase: A key regulator of energy balance with many roles in human disease. J Intern Med 276: 543-559, 2014.

23. Ahluwalia A and Tarnawski AS: Activation of the metabolic sensor-AMP activated protein kinase reverses impairment of angiogenesis in aging myocardial microvascular endothelial cells. Implications for the aging heart. J Physiol Pharmacol 62: 583-587, 2011.

24. Izumi Y, Shiota M, Kusakabe H, Hikita Y, Nakao T, Nakamura Y, Muro T, Miura K, Yoshiyama M and Iwao H: Pravastatin accelerates ischemia-induced angiogenesis through AMP-activated protein kinase. Hypertens Res 32: 675-679, 2009.

25. Shimano M, Ouchi N, Shibata R, Ohashi K, Pimentel DR, Murohara T and Walsh K: Adiponectin deficiency exacerbates cardiac dysfunction following pressure overload through disruption of an AMPK-dependent angiogenic response. J Mol Cell Cardiol 49: 210-220, 2010.

26. Su KH, Yu YB, Hou HH, Zhao JF, Kou YR, Cheng LC, Shyue SK and Lee TS: AMP-activated protein kinase mediates erythropoietin-induced activation of endothelial nitric oxide synthase. J Cell Physiol 227: 3053-3062, 2012.

27. Zheng S, Li W, Xu M, Bai X, Zhou Z, Han J, Shyy JY and Wang X: Calcitonin gene-related peptide promotes angiogenesis via AMP-activated protein kinase. Am J Physiol Cell Physiol 299: C1485-C1492, 2010.